Supporting Information

Sustained release of matrine via salt formation with hesperetin

Yujing Zhu,[ab] Xiaoju Shi,[c] Duanxiu Li[b], Shuang Li[d], Lin Wang[e], Zongwu Deng,[*ab] Shaohua Huang[df] and Hailu Zhang[*abg]

[a] School of Nano-Tech and Nano-Bionics, University of Science and Technology of China, Hefei 230026, P. R. China.

[b] Laboratory of Pharmaceutical Solid-State Chemistry, Suzhou Institute of Nano-Tech and Nano-Bionics, Chinese Academy of Sciences, Suzhou 215123, P. R. China.

[c] Suzhou Vocational Health College, Suzhou 215009, P.R. China.

[d] Institute of Drug Discovery Technology, Ningbo University, Ningbo 315211, P. R. China.

[e] Jiangsu Vocational College of Agriculture and Forestry, Jurong 212400, P. R. China.

[f] Qian Xuesen Collaborative Research Center for Astrochemistry and Space Life Sciences, Ningbo University, Ningbo 315211, P. R. China.

[g] Interdisciplinary Institute of NMR and Molecular Sciences (NMR-X), School of Chemistry and Chemical Engineering, Wuhan University of Science and Technology, Wuhan 430081, P. R. China.

[*] Corresponding Authors:

Tel.: +86-512-62872559; Fax: +86-512-62872559; E-mail: zwdeng2007@sinano.ac.cn.

Tel.: +86-512-62872713; Fax: +86-512-62603079; E-mail: hlzhang2008@sinano.ac.cn.

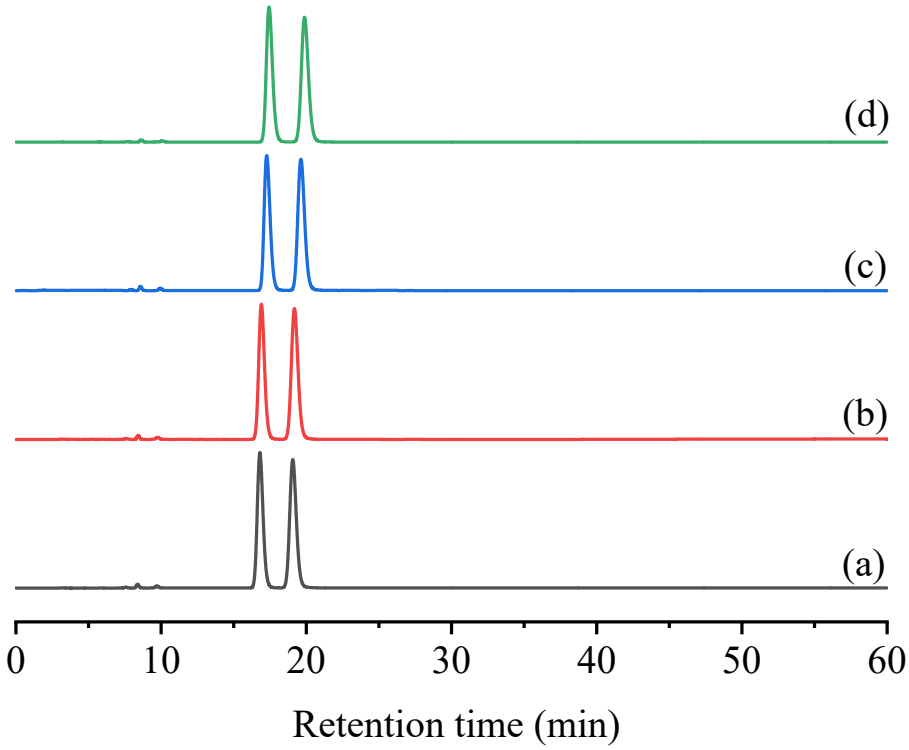

Fig. S1 The chiral HPLC spectra of HES (a), MAT–HES prepared by liquid-assisted grinding method (b), MAT–HES prepared by slurry method (c), and MAT–HES prepared by solvent evaporation (d).

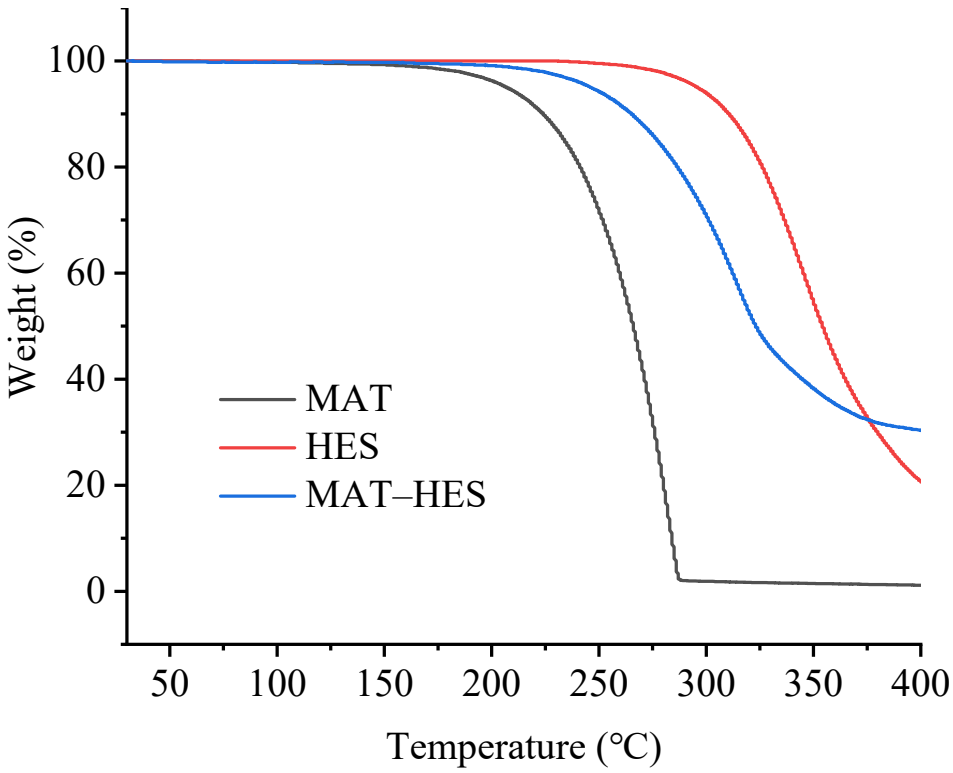

Fig. S2 TGA curves of MAT, HES, and MAT–HES.

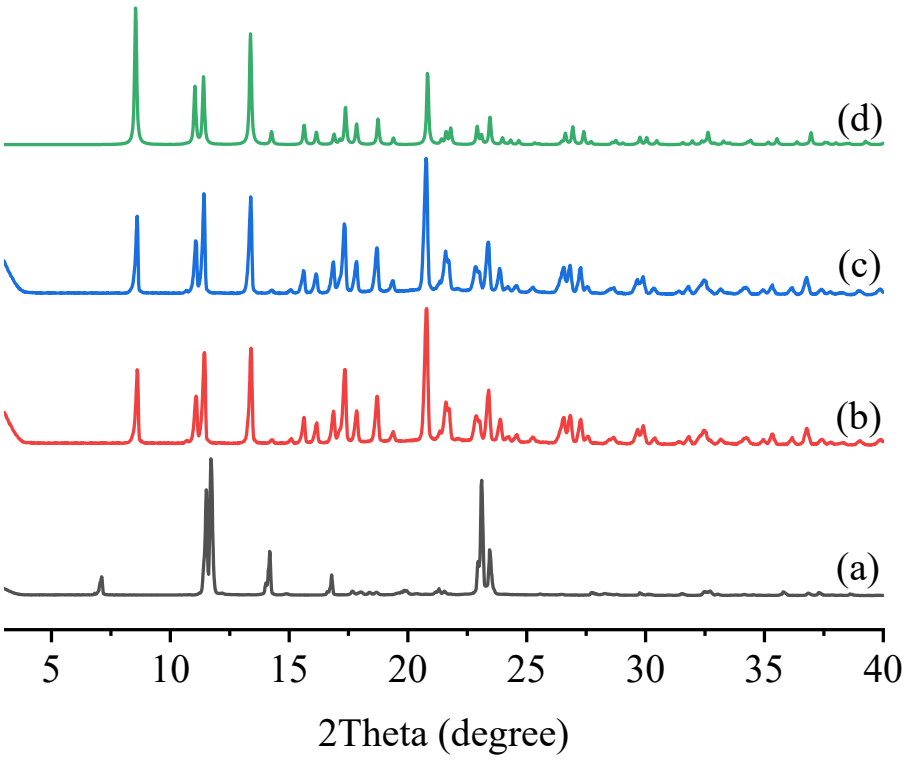

Fig. S3 Experimental powder XRD of MAT (a), its residual solids after the equilibrium solubility tests in pH 1.2 solution (b) and pH 6.8 PBS solution (c). The simulated powder XRD pattern of MAT hydrate (d) is provided for comparison.

Single crystal structure analysis of MAT–H_2O: MAT–H_2O crystallizes in a tetragonal system, $P4_32_12$ space group, with eight asymmetric units in a unit cell ($Z = 8$). Each asymmetric unit contains a MAT and 1.75 H_2O ($Z' = 1$, Fig. S4a). In the asymmetric unit, MAT and lattice water are connected via O2—H2C···N2 hydrogen bond (Fig. S4a), and the adjacent asymmetric units are linked and extend via O2—H2D···O1 hydrogen bond, forming an 1D chain structure (Fig. S4b).

Except for eight H_2O molecules existing in fixed positions, a solvent mask was calculated and 60 electrons were found in a void volume of 280 Å^3 per unit cell. This is consistent with the presence of 0.75[H_2O] per unit cell which account for 60 electrons per unit cell. Due to the highly disordered nature of these void H_2O molecules, they were squeezed out for clarity (Fig. S4c).

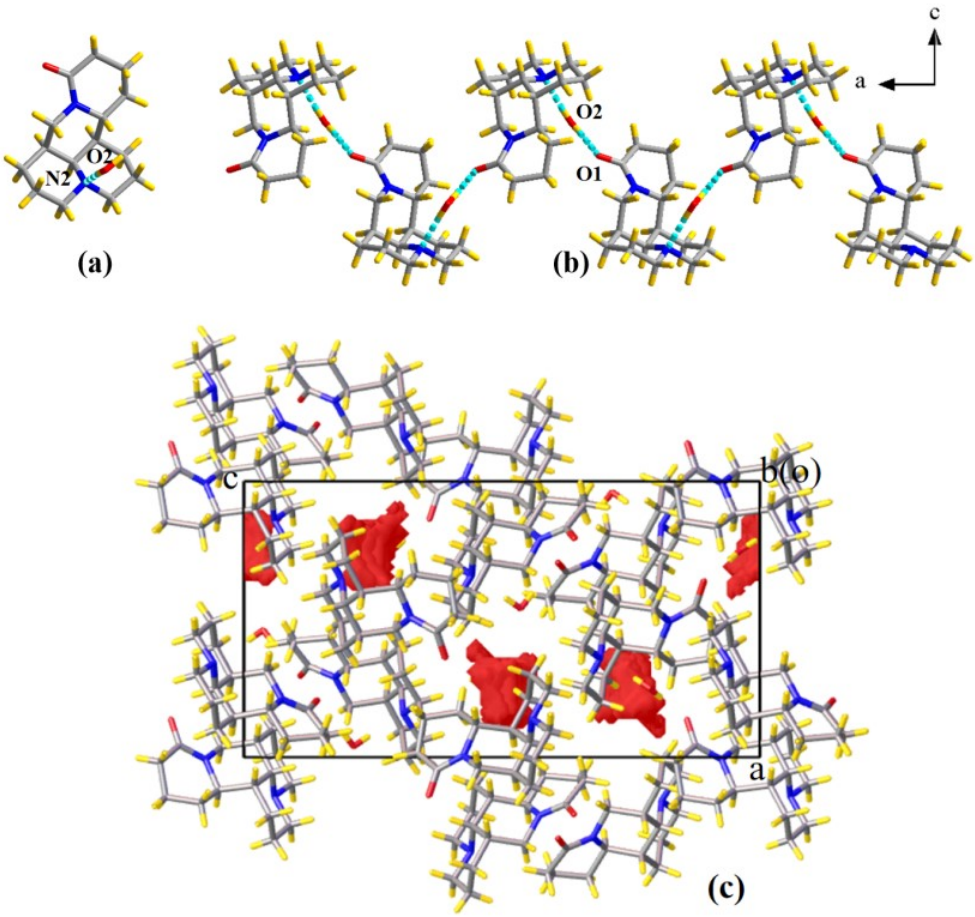

Fig. S4 The crystal structure of MAT–H_2O. The asymmetric unit (a, 0.75 disordered water not displayed), 1D molecular chain along the *a*-axis (b), 4 voids (red parts) in the unit cell (c).

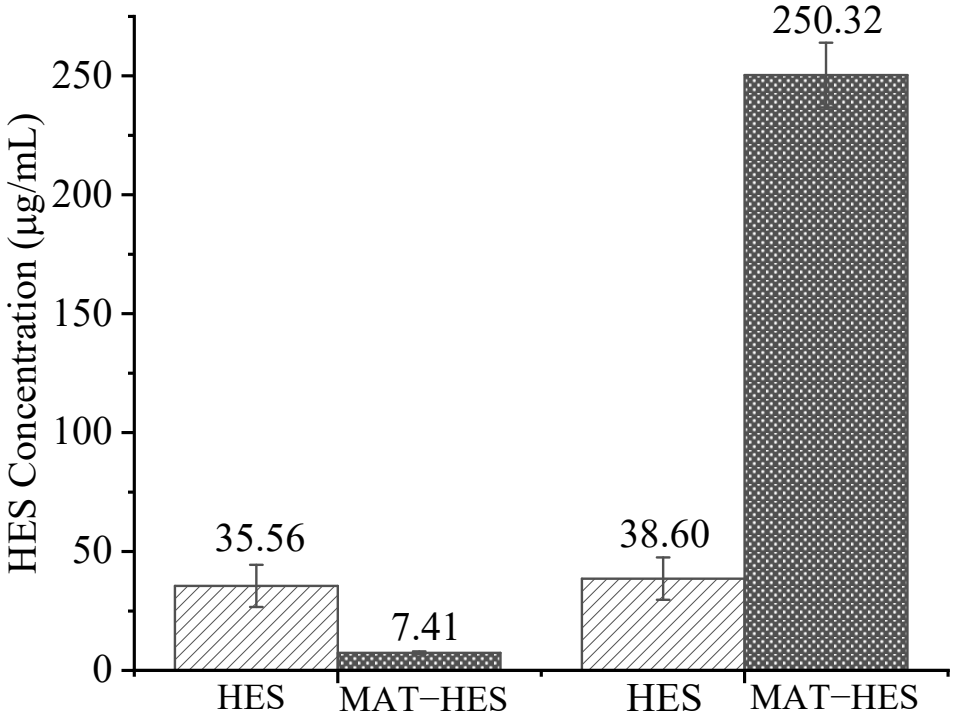

Fig. S5 Equilibrium solubilities of HES and MAT–HES in pH 1.2 HCl medium (left) and pH 6.8 PBS medium (right) at 37 °C.

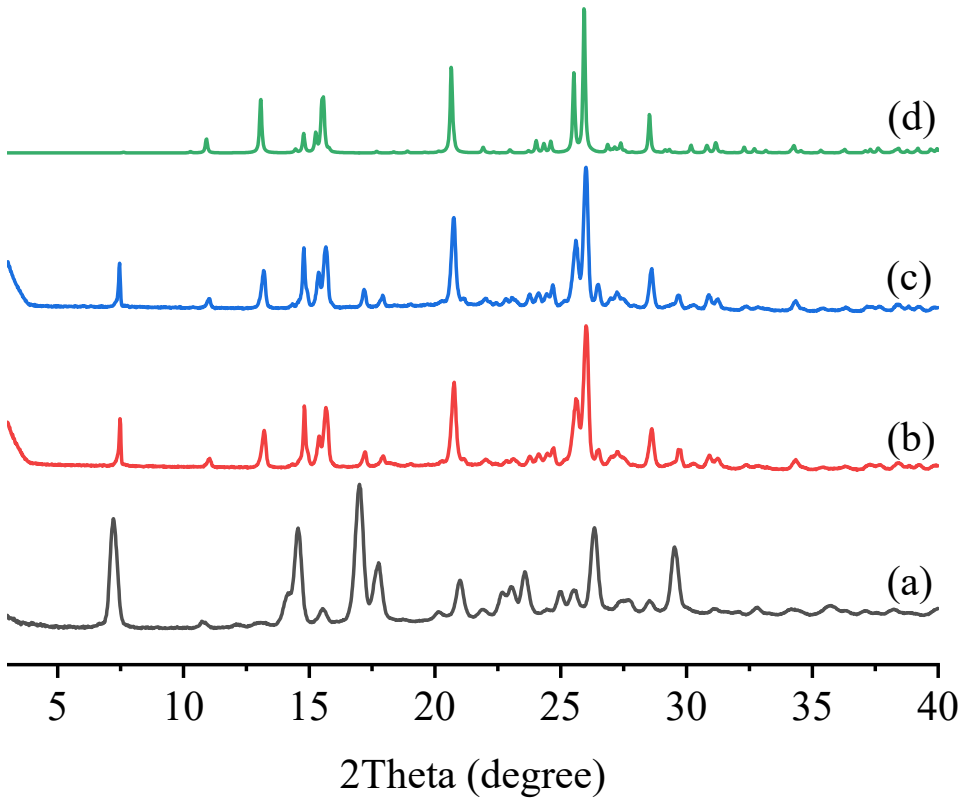

Fig. S6 Experimental powder XRD of HES (a), its residual solids after the equilibrium solubility tests in pH 1.2 solution (b) and pH 6.8 PBS solution (c). The simulated powder XRD pattern of HES monohydrate (d, CSD Refcode: FOYTOC) is provided for comparison.

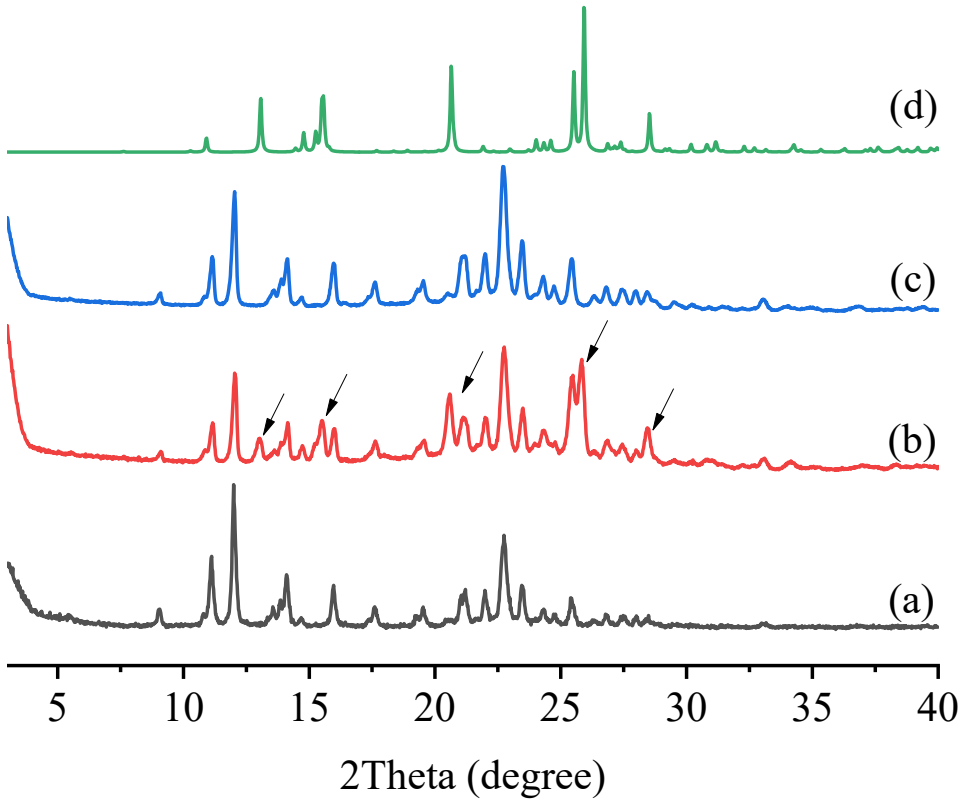

Fig. S7 Experimental powder XRD of MAT–HES (a), its residual solids after the equilibrium solubility tests in pH 1.2 solution (b) and pH 6.8 PBS solution (c). The simulated powder XRD pattern of HES monohydrate (d, CSD Refcode: FOYTOC) is also provided for comparison. For (b), the characteristic diffraction peaks of HES monohydrate were also marked.

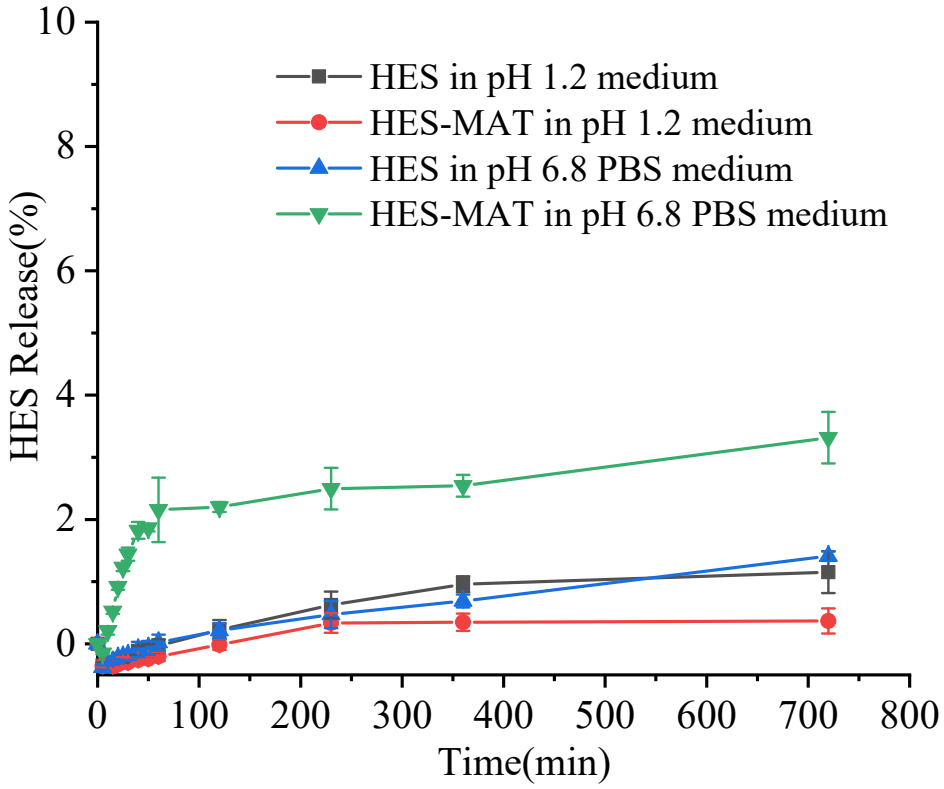

Fig. S8 Release profiles of HES in crystalline HES and MAT–HES in pH 1.2 HCl medium (a) and pH 6.8 PBS (b) at 37 °C.

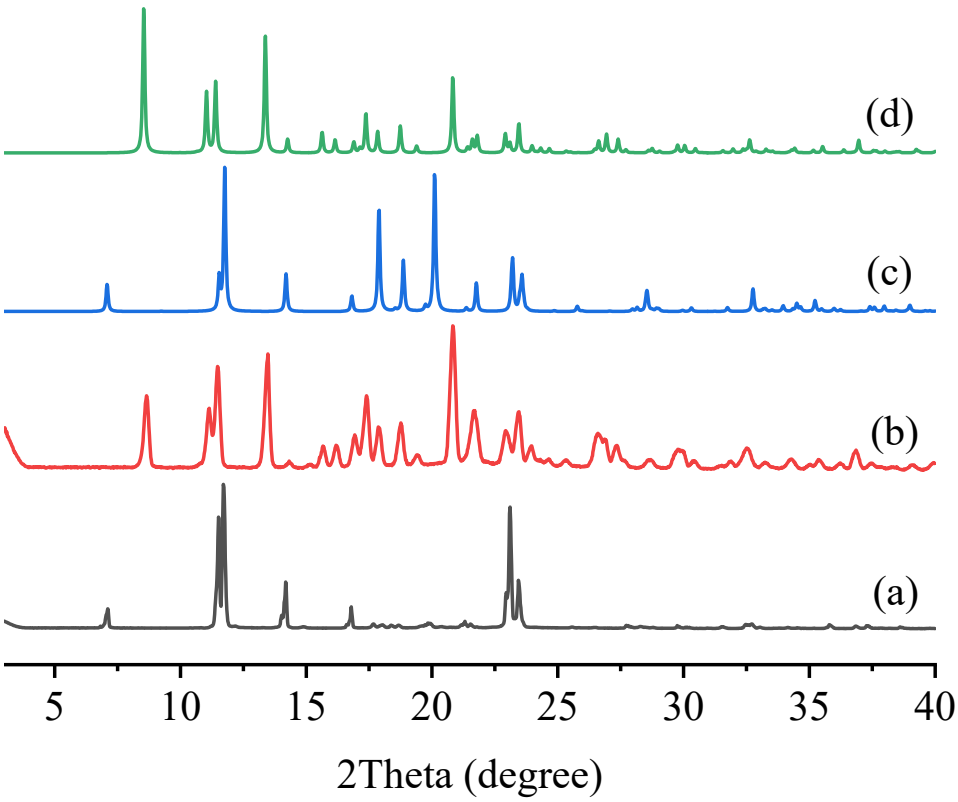

Fig. S9 Powder XRD patterns of MAT before (a) and after (b) equilibrating at 25 °C/90% RH condition. Simulated XRD patterns of MAT (c) and MAT–H_2O (d) are also provided for comparison.

Table S1 pH values after the solubility tests.

	pH 1.2	pH 6.8
MAT	10.19±0.31	9.35±0.08
HES	1.18±0.03	6.81± 0.17
MAT–HES	4.85±0.13	8.76±0.11